Obrabotka metallov (tekhnologiya, oborudovanie, instrumenty) = Metal Working and Material Science. 2021 vol. 23 no. 4 pp. 140–154
ISSN: 1994-6309 (print) / 2541-819X (online)
DOI: 10.17212/1994-6309-2021-23.4-140-154

NSTU NETI

Obrabotka metallov -
Metal Working and Material Science

Journal homepage: http://journals.nstu.ru/obrabotka_metallov

Stir zone material flow patterns during friction stir welding of heavy gauge AA5056 workpieces and stability of its mechanical properties

Tatiana Kalashnikova [1, 2, a, *], *Vladimir Beloborodov* [1, b], *Kseniya Osipovich* [1, c], *Andrey Vorontsov* [1, d], *Kirill Kalashnikov* [1, e]

[1] Institute of Strength Physics and Materials Science of Siberian Branch of Russian Academy of Sciences, 2/4, pr. Akademicheskii, Tomsk, 634055, Russian Federation
[2] National Research Tomsk State University, 36 Lenin ave., Tomsk, 634050, Russian Federation

[a] https://orcid.org/0000-0002-0388-4011, gelombang@ispms.tsc.ru, [b] https://orcid.org/0000-0003-4609-1617, vabel@ispms.ru,
[c] https://orcid.org/0000-0001-9534-775X, osipovich_k@ispms.ru, [d] https://orcid.org/0000-0002-4334-7616, vav@ispms.tsc.ru,
[e] https://orcid.org/0000-0002-0286-7156, kkn@ispms.tsc.ru

ARTICLE INFO

Article history:
Received: 16 September 2021
Revised: 28 September 2021
Accepted: 05 October 2021
Available online: 15 December 2021

Keywords:
Friction stir welding
Friction stir processing
Structural-phase state
Mechanical properties

Funding
The results were obtained in the framework of the Integrated Project “Establishment of production of high-tech large-sized equipment for intelligent adaptive friction stir welding for the aerospace and transport industries of the Russian Federation” (Agreement No. 075-11-2019-033 dated November 22, 2019) implemented by the NSTU and ISPMS SB RAS at the financial support of the Ministry of Education and Science of the Russian Federation as part of Decree of the Government of the Russian Federation No. 218 dated April 09, 2010.

ABSTRACT

Introduction. Friction stir welding and processing are almost identical processes of severe plastic deformation at elevated temperatures. These technologies differ mainly in the purpose of its use: the formation of a hardened surface layer or producing a welded joint. However, it is known that both during welding and during processing of heavy gauge workpieces temperature gradients occur. As a result, the conditions of adhesive interaction, material plastic flow, and the formation of the stir zone change as compared to thin-sheet workpieces with fundamentally different heat dissipation rates. In this connection, **the purpose of the work** is to determine the regularities of the structure formation and stability of the mechanical properties in different directions in the material of 35-mm-thick aluminum-magnesium alloy samples produced by friction stir welding/processing. **Research Methodology.** The technique and modes of friction stir welding and processing of AA5056 alloy workpieces with a thickness of 35 mm are described. Data on the equipment used for mechanical tests and structural research are given. **Results and discussion.** The data obtained show the excess mechanical properties of the processing zone material over the base metal ones in all studied directions. Material structure heterogeneities after friction stir welding/processing of heavy gauge workpieces have no determining effect on the stir zone properties. At the same time, there is no clear correlation between the tensile strength values and the load application direction, nor is there any significant difference in mechanical properties depending on the location of the samples inside the stir zone. The average ultimate tensile strength values in the vertical, transverse, and longitudinal directions are 302, 295 and 303 MPa, respectively, with the yield strength values of 155, 153 and 152 MPa, and the relative elongation of 27.2, 27.5, 28.7 %.

For citation: Kalashnikova T.A., Beloborodov V.A., Osipovich K.S., Vorontsov A.V., Kalashnikov K.N. Stir zone material flow patterns during friction stir welding of heavy gauge AA5056 workpieces and stability of its mechanical properties. *Obrabotka metallov (tekhnologiya, oborudovanie, instrumenty) = Metal Working and Material Science*, 2021, vol. 23, no. 4, pp. 140–154. DOI: 10.17212/1994-6309-2021-23.4-140-154. (In Russian).

*** Corresponding author**
Kalashnikova Tatiana A., Research Officer
Institute of Strength Physics and Materials Science
of Siberian Branch of Russian Academy of Sciences,
2/4, pr. Akademicheskii,
634055, Tomsk, Russian Federation
Tel.: 8 (382) 228-68-63, **e-mail:** gelombang@ispms.ru

Introduction

Friction Stir Welding (FSW) and Friction Stir Processing (FSP) are virtually identical processes of severe plastic deformation at elevated temperatures [1-3]. These technologies differ mainly in the purpose of their use: formation of a hardened surface layer or production of a welded joint. When a rotating tool is plunged into the workpiece and further moves, the material is heated and plastically deformed. During this process, the grain structure is fragmented, and then the transferred material cools down and simultaneously recrystallizes, resulting in significant changes in the material structure and its mechanical properties. These techniques are mainly used for welding or processing various aluminum alloys [4–16]. The most applicable are aluminum-magnesium alloys *AA5056* and *AA5083* [5, 7, 9, 12], alloys of the following systems: *Al-Mg-Sc*, *Al-Mg-Sc-Zr* [13, 15], *Al-Cu-Li* [11], *Al-Zn-Mg-Cu* [14, 16], *Al-Cu-Mg* [16], etc. It is also possible to produce joints and coatings based on dissimilar metals and alloys of *Al-Cu* [17], *Cu-Fe* [18], and other systems. It is also possible to form various reinforced metal matrix composite materials [18-20]. The technology of friction stir processing for hardening materials produced by additive technologies has a rather high degree of applicability [12, 18]. Friction stir welding can be performed both over the entire thickness of the workpiece and to adjust the depth of the processed area due to the size of the tool. Friction stir welding is possible with both butt and overlap welding and different types of bevelling before welding.

Depending on the thickness of the workpiece, the structure of the stir zone differs significantly: in large-thickness workpieces, a monolithic nugget is not formed, which is characteristic for *FSW*'ed or *FSP*'ed samples of 2–10 mm thickness. It is shown in detail on the example of *FSW* joint made of an alloy of the *Al-Mg-Sc-Zr* system with a thickness of 35 mm in [13]. In this case, due to the large workpiece thickness, temperature gradients, and the conditions of adhesion interaction, the plastic flow of the material and the formation of the stir zone change compared to the thin-sheet workpieces with fundamentally different heat dissipation characteristics. In this regard, one of the most relevant tasks for research is to determine the pattern of material flow along the tool contour and the formation of mechanical properties of the processed or welded material of large-thickness workpieces in different directions. This work aims to study the stability of the large-thickness sample formation and the homogeneity of its mechanical properties.

Methods

Friction stir welding and processing were carried out on a particular unit at *CJSC Cheboksary Enterprise "Sespel"*. For this purpose, 200 mm wide and 35 mm thick AA5056 alloy sheets were used. Processing/welding was carried out according to the scheme shown in Figure 1. Workpiece (1) was processed by tool (2), by penetration a pin (3) with rotation (4) of the tool, followed by movement along the joint line (5). This technique was used not to produce a weld joint but to determine the boundary values of the process parameters of intelligent adaptive friction stir welding for 35 mm thick plates. The rotational speed of the tool (ω) was 250 rpm, the longitudinal velocity (v) was 250 mm/min, the tool loading force to the workpiece (P) was 3,600 kg, and the tool inclination angle was 3.0 deg. The process parameters were selected experimentally. The processed area was 250 mm long. Specimens for mechanical tests were cut in area (6). Specimens from the processed area (7) were cut in the vertical direction (8), transverse direction (9), and longitudinal direction (10) in the number of eight samples for each direction. The size of the investigated area does not comply with the Interstate standards, so the samples were cut in a reduced shape, preserving the standard proportions. The size of the test specimens was 2.7×2.2×12 mm. A thin section (11) was cut out to investigate the cross-sectional structure of the processed material. In this case, the stir zone (12) and the heat and thermomechanically affected zones (13) are clearly distinguished in the section.

Sections for the study of changes in the structure by thickness were cut from the workpiece in the horizontal plane after friction stir processing on an electric discharge machine in a planar section. Then the sections were divided into two parts (Figure 2) to study the area where the tool enters the workpiece (speci-

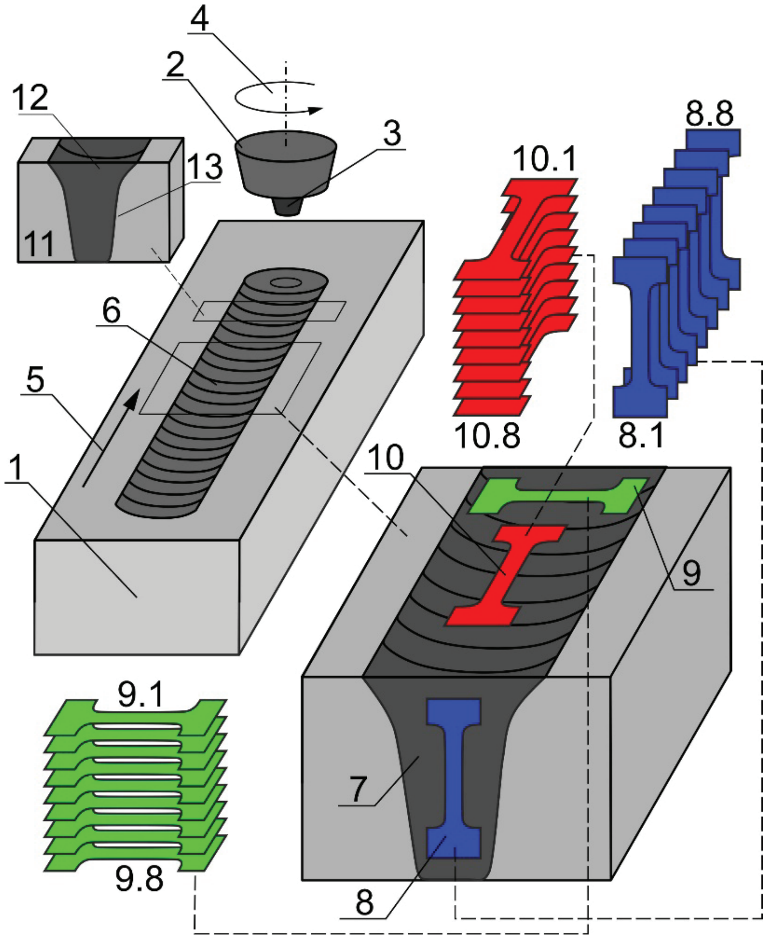

Fig. 1. Scheme of the friction stir welding process and cutting out samples for mechanical tests and metallography:

1 – workpiece; *2* – tool; *3* – tool pin; *4* – direction of tool rotation; *5* – direction of friction stir processing/welding; *6* – cutting area of the specimens for mechanical tests; *7* – processing zone; *8* – cutting of the blade-shaped test specimens in the vertical direction; *9* – cutting of the blade-shaped test specimens in transverse direction; *10* – cutting of the blade-shaped test specimens in longitudinal direction; *11* – metallographic sections; *12* – stir zone; *13* – thermomechanically affected and heat affected zones

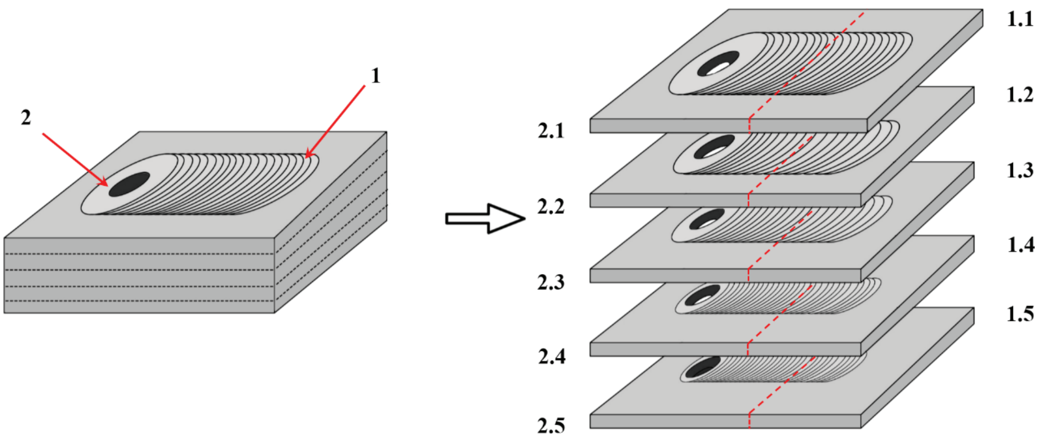

Fig. 2. Scheme of cutting out samples in horizontal section to study the material plastic flow in the stir zone through the thickness of the processed material:

1 – tool inlet zone; *2* – tool outlet zone mens 1.1–1.5) and the zone with a tool outlet hole (specimens 2.1–2.5). Changes in the microstructure of the metal were studied on polished and etched sections using a metallographic microscope *ALTAMI MET 1C*. Mechanical tests were carried out on a universal testing machine *UTS 110M-100*. Microhardness was measured on a *Duramin* 5 microhardness tester.

Results and discussion

During friction stir welding or processing, a complex structure is formed in the stir zone along with the entire thickness of the workpiece to the depth of tool plunge, which is the result of the formation of material flows along the tool contour (Figure 3). A typical monolithic nugget was not formed in the stir zone of the *AA5056* sample with a thickness of 35 mm. However, several nuggets were formed in swirling layers under the tool shoulders and at the root of the stir zone (Figure 3). A similar pattern was observed when analyzing the structure of *Al-Mg-Sc-Zr* alloy in [13]. But, due to more qualitatively selected process parameters at the stage of preliminary studies in this work, it was possible to avoid significant discontinuities in the upper part of the sample. The modes were selected so that defects are not formed in the processed area, which is often encountered during welding large-thickness workpieces. The dotted lines highlight the distinct structural zones created in the *FSW* joints: stir zone (1), thermomechanically affected zone (2), heat affected one (3), and base metal (4). The thermomechanically affected zone on the advancing side (*AS*) has a sharp boundary with the stir zone, but on the retreating side (*RS*), there is a smooth transition from the thermomechanically affected zone to the weld.

The macrostructure of the samples in the horizontal section is shown in Figures 4 and 5. In the upper part of the stir zone, one can distinguish a significant structural heterogeneity (4 in Figure 4, *a*). This pattern may be related to the plastic deformation effect on the upper part of the sample structure by the tool shoulders during processing. In the zone of the movement started, inhomogeneity of the structure is formed in all areas along with the joint thickness (1 in Figures 4 and 5). It is connected with rather complicated

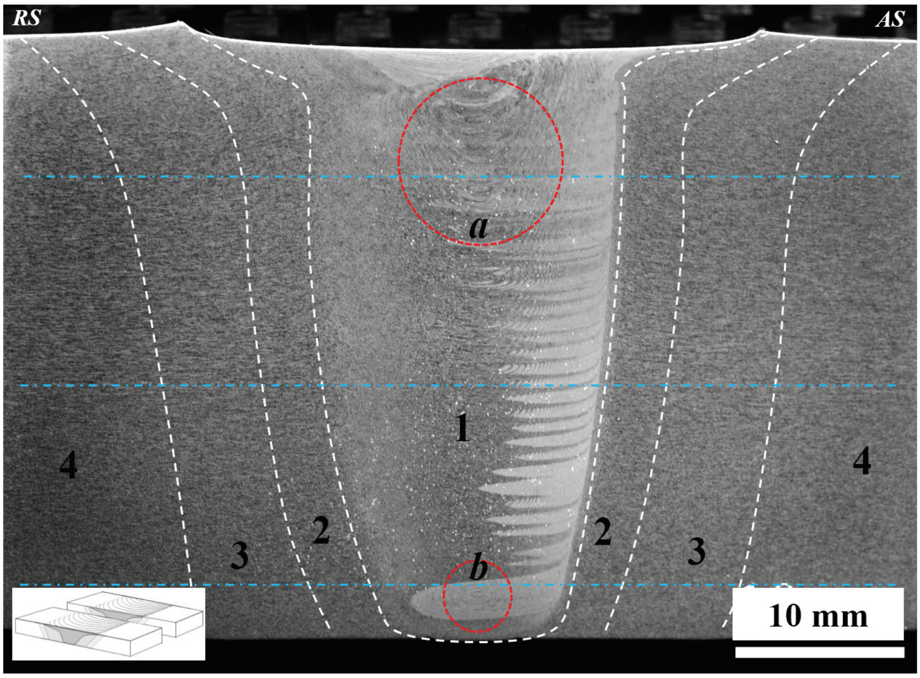

Fig. 3. Macrostructure of a sample cut in cross section after friction stir processing:

1 – stir zone; *2* – thermomechanically affected zone; *3* – heat affected zone; *4* – base metal; *a* – nugget formation in the near-shoulder area; *б* – nugget formation in the weld root; RS – retreating side; AS – advancing side. Lines along which the microhardness measurement was carried out are indicated with dashed lines

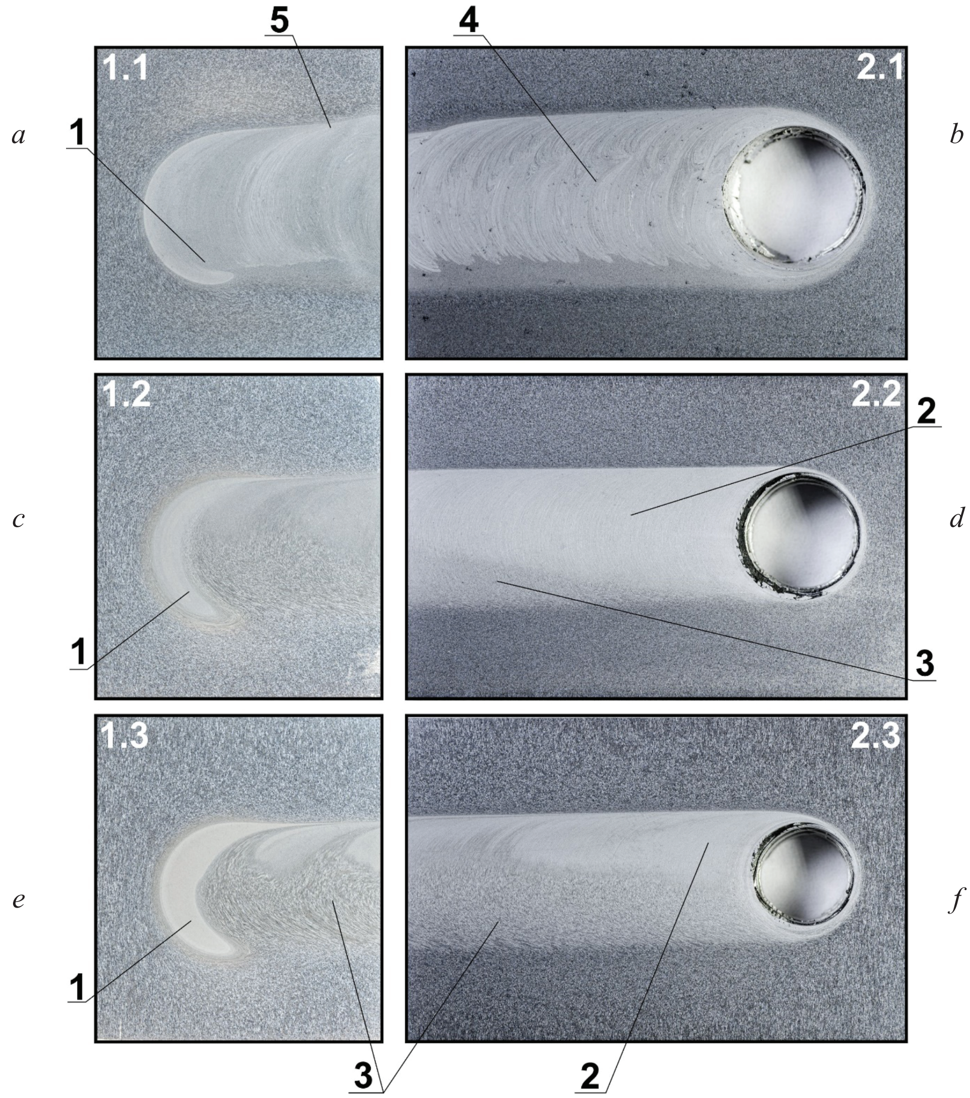

Fig. 4. Macrostructure of samples 1.1 – 1.3 (*a, c, e*) and 2.1 – 2.3 (*b, d, f*) cut in the horizontal section according to the scheme shown in Fig. 1:

1 – inhomogeneities of material structure in the tool inlet zone; *2* – area with a predominantly etched structure with a layered structure of the stir zone; *3* – area with predominantly etched grains in the stir zone; *4* – inhomogeneities of the stir zone structure in the near-shoulder area; *5* – change in the width of the processing zone at the beginning of the tool movement

conditions at the beginning of tool movement due to unsteady thermal mode. Further along the weld length, a thickening of the stir zone (5 in Figure 4) can be distinguished. In such an area, after heating the material, the tool fully presses the shoulders against the workpiece and forms a stir zone of the width that should be formed at the steady welding/processing mode stage.

In the lower layers, the metal structure at the steady-state stage is formed with more excellent stability over the length of the weld (Figure 4, *b*, *c*). In the horizontal section samples after etching, two types of structure are distinguished, containing elements with different etching characters. In the first (2 in Figures 4 and 5), the layers of transferred metal are well defined, and the distance between them correlates with the value of the feed per tool revolution. In the second region, the structure shows a tendency to etch on the grain (3 in Figures 4, 5) and does not show a layered structure of the stir zone.

In the lower part of the stir zone (Figure 5a,b), the metal structure is represented by a relatively stable structure. There are also zones where etching reveals layers (2 in Figure 5) and grains (3 in Figure 5) in the stir zone. It has to be noted that the distribution of these zones along the thickness of samples is rather inhomogeneous and changes from one sample to another irregularly. In general, in the lower layers of the

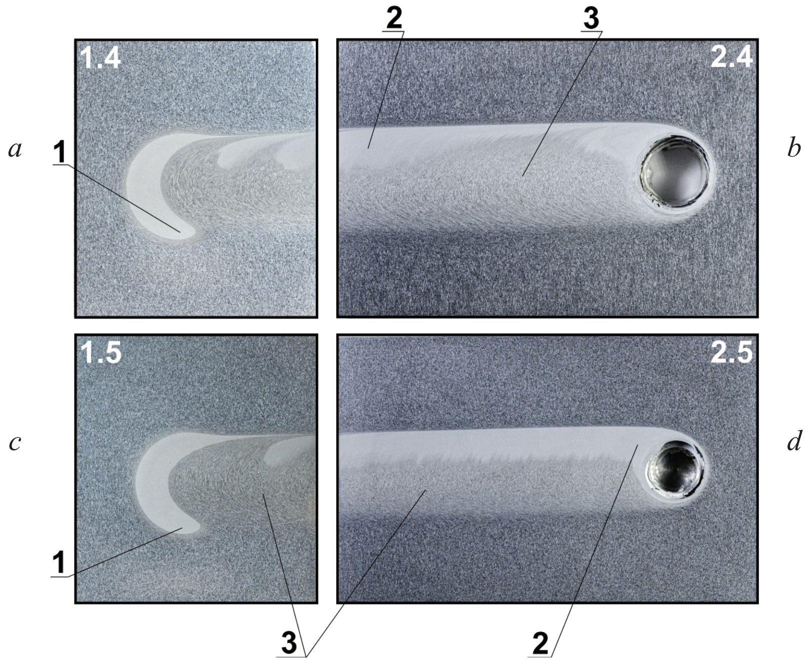

Fig. 5. Macrostructure of samples 1.4–1.5 (*a, c*) and 2.4–2.5 (*b, d*) cut in the horizontal section according to the scheme shown in Fig. 1:
1 – inhomogeneities of material structure in the tool inlet zone; *2* – area with a predominantly etched layered structure of the stir zone; *3* – area with predominantly etched grains in the stir zone

sample, the structure of the stir zone is more homogeneous than in the upper layers. This position may explain more significant pressure from the welding tool pressing at the bottom of the stir zone than at the top. In part, the mechanics of the welding/processing procedure can confirm this.

The structure in the tool inlet zone has a similar structure in all areas throughout the thickness of the sample (Figure 6). As can be seen from Figure 6 *a-d*, the structure is represented by a mixture of etched layers and etched grains. The heterogeneities in the structure appear clearly in the form of complex shapes in the stir zone organization (Figure 6 *b,e*). The size of the layers is close to the amount of feed per revolution during tool movement. The reason why etching shows layers in some areas and grains in others is not completely clear. It can be assumed that the etchability of the grain boundaries is less than the etchability of the transfer layers at the boundary of the metal flows that form the joint, while the etchability of the grain boundaries is higher inside the flows. No weld defects characteristic of friction stir welding was detected in the structure of the samples, which may indicate potentially high mechanical properties of the material in different directions.

In the tool outlet zone (Figures 7, 8), the structure of the metal, on the contrary, significantly depends on the distance from the tool shoulders. In the upper part of the sample (near the shoulders), one can see the structure of inhomogeneities described earlier in the macrostructural analysis (Figure 7 *a*). Different structural patterns at various depths can be identified in the shape and size of the transfer layer and the features of its state in the tool outlet zone (Figure 7 *c-e*, Figure 8 *a-d*). The most negligible thickness of the transfer layer and the stir zone is expected to be in the lower part of the processed area, where the tool pin diameter is minimal (Figures 8 *c, d*). There are also transfer layers partially detached from the stir zone at almost every level throughout the height of the sample (Figures 7 *c-e*, Figure 8 *a*). The adhesion of aluminum alloy causes the detachment of the stir zone part at tool output to the steel tool and the fact that quite a large portion of the material during processing is between the fillets of screw pin.

Determination of the weld and near-weld material microhardness shows that in the main structural zones of the 35 mm thick *AA5056* sample, there is no material hardening as compared to the base metal value for the corresponding alloy (Fig. 9). The data obtained during *Vickers* microhardness measurements of the

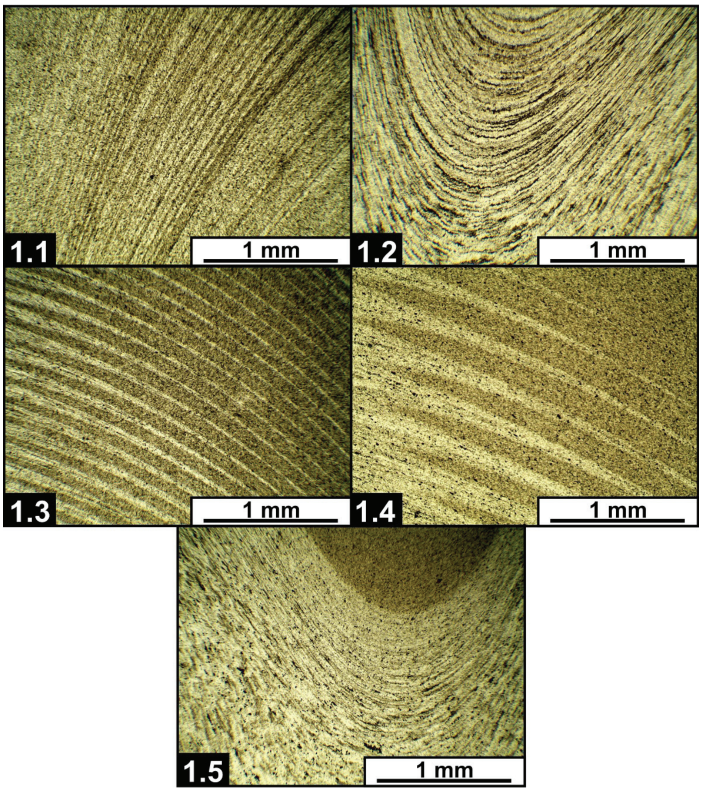

a *b* *c* *d* *e*

Fig. 6. Structure of samples 1.1–1.5 (*a–e*) in the tool inlet zone, cut in the horizontal section according to the scheme shown in Fig. 1

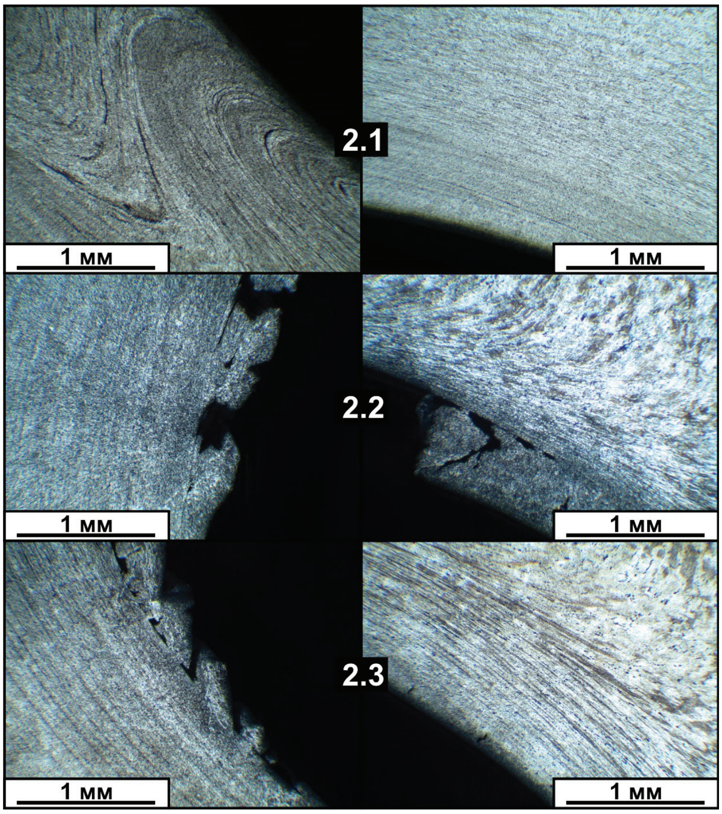

a *b* *c* *d* *e* *f*

Fig. 7. Structure of samples 2.1 (*a, b*), 2.2 (*e, f*) and 2.3 (*∂, e*) in the tool outlet zone, cut in the horizontal section according to the scheme shown in Fig. 1

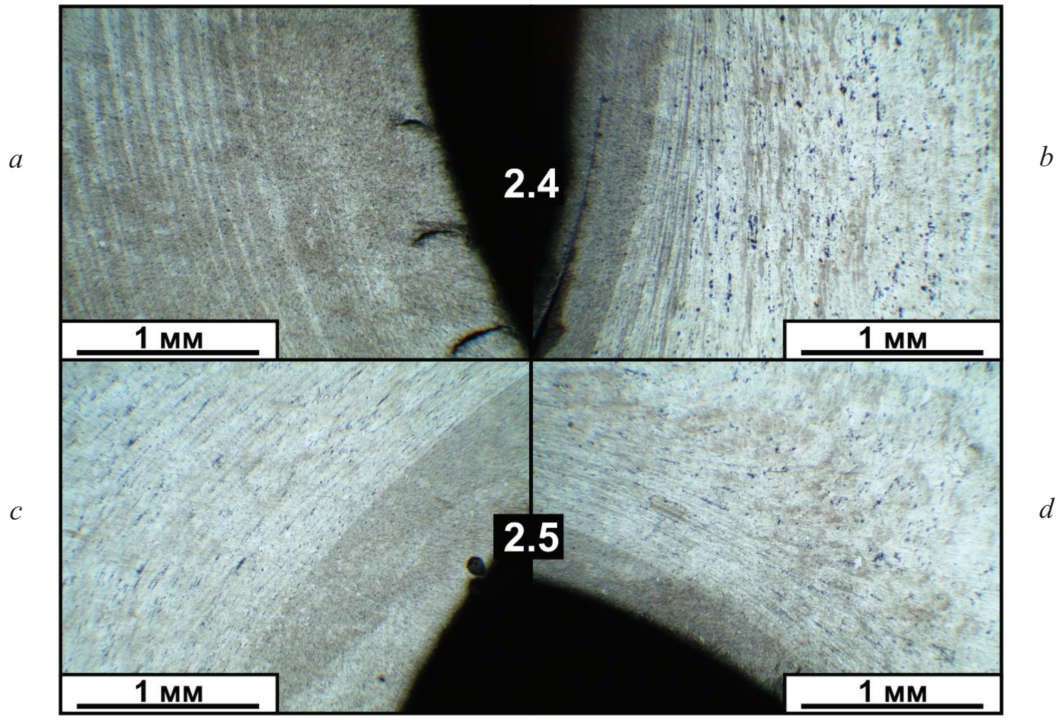

Fig. 8. Structure of samples 2.4 (*a, b*) and 2.5 (*c, d*) in the tool outlet zone, cut in the horizontal section according to the scheme shown in Fig. 1

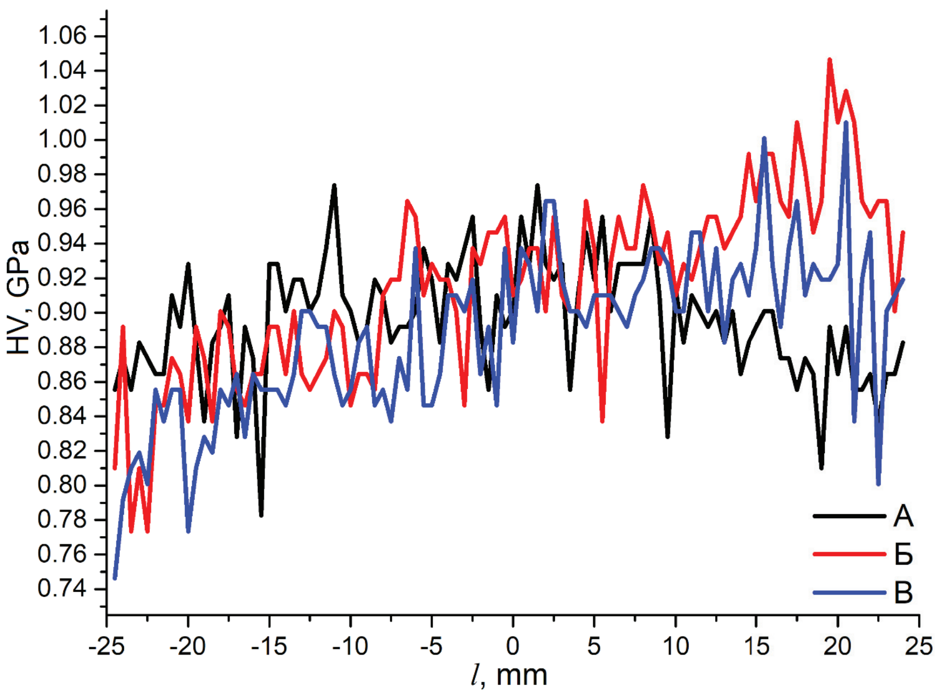

Fig. 9. Change of microhardness measured according to the scheme shown in Fig. 2 in the stir zone and near-weld zone

main structural zones also show the absence of significant hardening of the material and slight differences in the hardness values in the different thickness sections of the joint. Thus, scatter of microhardness values on the whole sample is essential (from 745 to 1045 MPa, i.e., 40 % from the minimum value), which is much higher than an increase of microhardness in the central part of the stir zone (from 745 to 975 MPa or 31 % from the minimum value) concerning microhardness of base metal.

Mechanical tests of the specimens cut in different directions from the stir zone (scheme in Figure 1) show typical deformation behavior for aluminum-magnesium alloys with an inherent discontinuous ductility effect (Figure 10). Tests of the base metal of workpieces show average ultimate tensile strength values of 301 MPa. Mechanical tests showed that the samples are characterized by sufficiently high mechanical properties in the vertical (Figure 10a), transverse (Figure 10b), and longitudinal (Figure 10c) directions compared with the characteristics of the base metal. The average values of the ultimate tensile strength in the vertical, transverse, and longitudinal directions are 302 MPa, 295 MPa, and 303 MPa, the yield strength is 155 MPa, 153 MPa, and 152 MPa, and the relative elongation is 27.2 %, 27.5 %, and 28.7 %, respectively. In addition to sufficiently close values of tensile strength, yield strength, and ductility, high stability of deformation behavior under tension can also be noted for the samples, as evidenced by the overlap of the graphs with each other.

Evaluation of the tensile strength stability for different loading directions (Figure 11) allows specifying that in general, in the transverse direction, the strength properties are somewhat lower in all measurement areas, but, in all testing directions, the strength of the weld material is higher than the strength of the original sheet metal. In the joint central part, there is also some tendency for the mechanical strength to decrease compared to the values at the top and bottom areas.

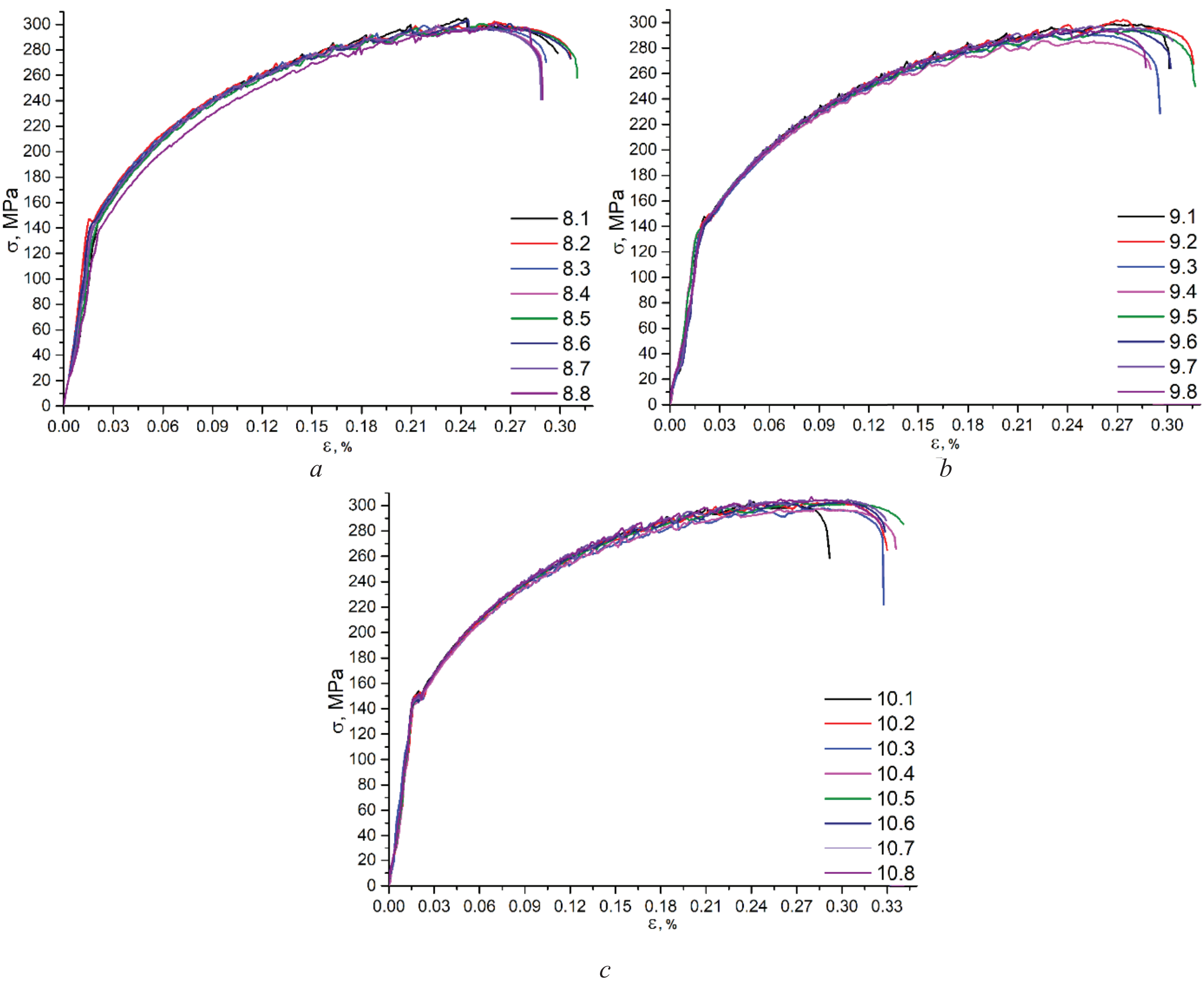

Fig. 10. Test diagrams for specimens cut in vertical (*a*), transverse (*b*) and longitudinal (*c*) directions according to the scheme shown in Fig. 1

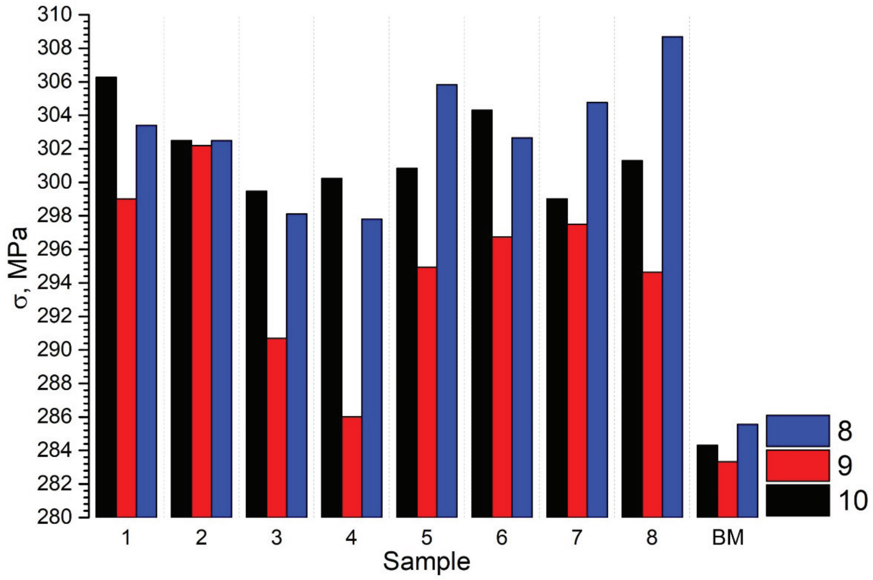

Fig. 11. Comparison of the ultimate tensile strength of test samples cut from different areas of the stir zone with the base metal one

Conclusion

The conducted studies show that despite inhomogeneities in the structure of the samples produced by friction stir processing of 35 mm thick workpieces, the mechanical properties of the stir zone material exceed the base metal values in all directions relative to the processing line. Material structure heterogeneities after friction stir welding/processing have no determining influence on the material properties of the stir zone. There is no clear correlation between the strength values and the direction of load application, nor is there any significant difference in mechanical properties depending on the location of the specimens within the stir zone. The average ultimate tensile strength values in the vertical, transverse, and longitudinal directions are 302 MPa, 295 MPa, and 303 MPa, yield strength – 155 MPa, 153 MPa, and 152 MPa, and ductility – 27.2 %, 27.5 %, and 28.7 % respectively. The deformation behavior of the specimens during the tests is similar, and only small differences in the process of plastic deformation and fracture can be distinguished for each group of ones. Microhardness values are also quite close and show no tendency to increase or decrease in the stir zone by more than 31 %, while the scatter of microhardness values for the sample as a whole is about 40 %. The obtained data allow concluding the high degree of applicability of friction stir welding and friction stir processing technologies to produce permanent joints and hardened surface structures of workpieces made of aluminum-magnesium alloy *AA5056*, including heavy gauge ones.

References

1. Mishra R.S., Ma Z.Y. Friction stir welding and processing. *Materials Science and Engineering: R: Reports*, 2005, vol. 50, iss. 1, pp. 1–78. DOI: 10.1016/j.mser.2005.07.001.

2. Threadgill P.L., Leonard A.J., Shercliff H.R., Withers P.J. Friction stir welding of aluminium alloys. *International Materials Reviews*, 2009, vol. 54, iss. 2, pp. 49–93. DOI: 10.1179/174328009X411136.

3. Balasubramanian V. Relationship between base metal properties and friction stir welding process parameters. *Materials Science and Engineering: A.*, 2008, vol. 480, iss. 1–2, pp. 397–403. DOI: 10.1016/j.msea.2007.07.048.

4. Deng Y., Peng B., Xu G., Pan Q., Yin Z., Ye R., Wang Y., Lu L. Effects of Sc and Zr on mechanical property and microstructure of tungsten inert gas and friction stir welded aerospace high strength Al-Zn-Mg alloys. *Materials Science and Engineering: A.*, 2015, vol. 639, pp. 500–513. DOI: 10.1016/j.msea.2015.05.052.

5. Han M.S., Lee S.J., Park J.C., Ko S.C., Woo Y.B., Kim S.J. Optimum condition by mechanical characteristic evaluation in friction stir welding for 5083-O Al alloy. *Transactions of Nonferrous Metals Society of China*, 2009, vol. 19, pp. 17–22. DOI: 10.1016/S1003-6326(10)60238-5.

6. Miranda A.C.O., Gerlich A, Walbridge S. Aluminum friction stir welds: Review of fatigue parameter data and probabilistic fracture mechanics analysis. *Engineering Fracture Mechanics*, 2015, vol. 147, pp. 243–260. DOI: 10.1016/j.engfracmech.2015.09.007.

7. Chennaiah M.B., Kumar K.R., Sridhar V. Influence of tool profiles on similar Al-5083 alloys using friction stir welding. *Materials Today: Proceedings*, 2021, vol. 46, pp. 8032–8037. DOI: 10.1016/j.matpr.2021.02.787.

8. Sabari S.S., Malarvizhi S, Balasubramanian V. Characteristics of FSW and UWFSW joints of AA2519-T87 aluminium alloy: Effect of tool rotation speed. *Journal of Manufacturing Processes*, 2016, vol. 22, pp. 278–289. DOI: 10.1016/j.jmapro.2016.03.014.

9. Koilraj M., Sundareswaran V., Vijayan S., Koteswara Rao S.R. Friction stir welding of dissimilar aluminum alloys AA2219 to AA5083 – Optimization of process parameters using Taguchi technique. *Materials and Design*, 2012, vol. 42, pp. 1–7. DOI: 10.1016/j.matdes.2012.02.016.

10. Khan N.Z., Maqbool A., Ahmad T., Siddiquee A.N., Khan Z.A. Fracture behaviour of friction stir welded dissimilar aluminium alloys. *Materials Today: Proceedings*, 2020, vol. 46, pp. 6688–6691. DOI: 10.1016/j.matpr.2021.04.158.

11. Naumov A., Isupov F., Rylkov E., Polyakov P., Panteleev M., Skupov A., Amancio-Filho S.T., Panchenko O. Microstructural evolution and mechanical performance of Al-Cu-Li alloy joined by friction stir welding. *Journal of Materials Research and Technology*, 2020, vol. 9, iss. 6, pp. 14454–14466. DOI: 10.1016/j.jmrt.2020.10.008.

12. Kalashnikova T.A., Chumaevskii A.V., Rubtsov V.E., Kalashnikov K.N., Kolubaev E.A., Eliseev A.A. Structural heredity of the aluminum alloy obtained by the additive method and modified under severe thermomechanical action on its final structure and properties. *Russian Physics Journal*, 2020, vol. 62, iss. 9, pp. 1565–1572. DOI: 10.1007/s11182-020-01877-z.

13. Kalashnikova T., Chumaevskii A., Kalashnikov K., Fortuna S., Kolubaev E., Tarasov S. Microstructural analysis of friction stir butt welded Al-Mg-Sc-Zr alloy heavy gauge sheets. *Metals*, 2020, vol. 10, iss. 6, pp. 1–20. DOI: 10.3390/met10060806.

14. Orozco-Caballero A., Ruano O.A., Rauch E.F., Carreño F. Severe friction stir processing of an Al-Zn-Mg-Cu alloy: Misorientation and its influence on superplasticity. *Materials and Design*, 2018, vol. 137, pp. 128–139. DOI: 10.1016/j.matdes.2017.10.008.

15. Xie J., Chen X.P., Mei L., Ren P., Huang G.J., Liu Q. Multifractal analyses of serrated flow in friction stir processed Al–Mg–Sc alloy. *Materials Science and Engineering: A*, 2020, vol. 786, p. 139436. DOI: 10.1016/j.msea.2020.139436.

16. Anil Kumar K.S., Murigendrappa S.M., Kumar H. A bottom-up optimization approach for friction stir welding parameters of dissimilar AA2024-T351 and AA7075-T651 alloys. *Journal of Materials Engineering and Performance*, 2017, vol. 26, iss. 7, pp. 3347–3367. DOI: 10.1007/s11665-017-2746-z.

17. Zykova A., Chumaevskii A., Gusarova A., Kalashnikova T., Fortuna S., Savchenko N., Kolubaev E., Tarasov S. Microstructure of in-situ friction stir processed Al-Cu transition zone. *Metals*, 2020, vol. 10, iss. 6, p. 818. DOI: 10.3390/met10060818.

18. Gusarova A.V., Chumaevskii A.V., Osipovich K.S., Kalashnikov K.N., Kalashnikova T.A. Regularities of structural changes after friction stir processing in materials obtained by the additive method. *Nanoscience and Technology: An International Journal*, 2020, vol. 11, iss. 3, pp. 195–205. DOI: 10.1615/NanoSciTechnolIntJ.2020033694.

19. Zykova A.P., Tarasov S.Yu., Chumaevskiy A.V., Kolubaev E.A. A review of friction stir processing of structural metallic materials: process, properties, and methods. *Metals*, 2020, vol. 10, iss. 6, p. 772. DOI: 10.3390/met10060772.

20. Chaudhary A., Kumar Dev A., Goel A., Butola R., Ranganath M.S. The mechanical properties of different alloys in friction stir processing: a review. *Materials Today: Proceedings*, 2018, vol. 5, iss. 2, pp. 5553–5562. DOI: 10.1016/j.matpr.2017.12.146.

Conflicts of Interest

The authors declare no conflict of interest.